

THESIS

SEISMIC FRAGILITY ANALYSIS OF REINFORCED MASONRY BUILDINGS

Submitted by

José Efraín Mazariegos Zamora

Department of Civil and Environmental Engineering

In partial fulfillment of the requirements

For the Degree of Master of Science

Colorado State University

Fort Collins, Colorado

Summer 2013

Master's Committee:

Advisor: John W. van de Lindt

Rebecca Atadero
Kelly Strong

ABSTRACT

SEISMIC FRAGILITY ANALYSIS OF REINFORCED MASONRY BUILDINGS

Reinforced masonry walls are a widely used lateral force resisting system for buildings around the world. These structures, if not correctly detailed to resist earthquake loads, are a main cause of casualties and economic losses, particularly in developing countries.

This thesis presents the result of a study whose objective was to apply the seismic fragility methodology to both in-plane (shear) and out-of-plane (transverse) reinforced masonry shear walls to quantify probabilities of exceedance for ASCE 41-06 drifts associated with continued occupancy, life safety, and collapse prevention, performance states.

The load-displacement curves (hysteresis) were obtained from quasi-static out-of-plane and in-plane experimental testing by Klingner et al. (2010). In this thesis, that data was applied to obtain the parameters for a widely used ten-parameter hysteretic model. The software SAPWood Version 2.0 was selected for use in this thesis to enable nonlinear modeling of the shear wall and out-of-plane components.

An analytical model of the reinforced masonry walls was developed in SAPWood and subjected to each earthquake within a well-known suite of 22 earthquakes. The peak of drifts for each ground motion record was recorded and each earthquake intensity increased over the range of interest, i.e. an incremental dynamic analysis (IDA) was performed. Finally, as mentioned the information obtained from the IDA was used to develop fragility curves for the in-plane and out-of-plane walls based on peak story drift limits defined in ASCE 41 for continued occupancy, life safety, and collapse prevention.

TABLE OF CONTENTS

ABSTRACT.....	ii
TABLE OF CONTENTS.....	iii
Chapter 1: Introduction.....	1
1.1 History and Evolution of Masonry	1
1.2 Seismic Risk Analysis.....	2
1.3 Fragility Analysis and its Graphical Representation	4
Chapter 2: Data and Modeling Fit	7
2.1 Network for Earthquake Engineering Simulation (NEES) Data for Masonry	7
2.1.1 Background and Scope.....	7
2.1.2 Existing Data on Reinforced Concrete Masonry Specimens with Clay Masonry Veneer.	7
2.1.3 Database used for Thesis.....	10
2.2 Modeling Approach	14
2.2.1 Hysteretic Behavior.....	14
2.2.2 Hysteretic Modeling.....	15
2.3 Modeling of Masonry Walls	18
2.4 Fragility Curves	22
Chapter 3: Modeling of a Low-Rise Reinforced Masonry Building	24
3.1 Modeling of Out-of-Plane Walls	27
3.2 Modeling of In-Plane Walls.....	28
Chapter 4: Fragility Analysis of the low-rise reinforced masonry walls	30
4.1 Damage Measures.....	30

4.2 Ground Motions	31
4.3 Construction of Fragility Curves	32
4.4 Discussion	38
Chapter 5: Conclusions	39
References	40

Chapter 1: Introduction

1.1 History and Evolution of Masonry

Since the beginning of modern civilization, masonry structures have been built not only for homes but also for aesthetic churches and arenas. Stone was the first masonry unit and was used for primitive structures. The Stonehenge ring on England's Salisbury Plains is 4000 years old, and is an example of ancient structures composed of masonry. The Egyptian pyramids in Giza, the Great Wall of China, the pyramids of Yucatan and Teotihuacan in Mexico, the stone walls at Machu Pichu (Figure 1.1), The Taj Mahal are all ancient structures highlighting the use of masonry over the centuries. In the United States, masonry has been used as one of the primary building materials for construction since the 18th century.



Figure 1.1 Machu Pichu Stone Walls, Peru.

Photograph by Danielle Lankhaar, My Shot for National Geographic Society ©

The concrete masonry unit (CMU) has a recent origin and can be found at the beginning of the 20th century, when Frank Lloyd Wright did his first experiments manufacturing concrete units [Huxtable, 2004]. Wright was looking for plasticity and a mechanism to add an unconventional texture to the walls. Over the years, these units became popular as a low cost alternative for buildings because of their ability to be modular while providing aesthetics.

Many masonry structures are designed to support only gravity loads. Due to their massive dead loads from the thick and heavy walls, the unreinforced structures were felt to be somewhat stable against lateral forces. With the development of construction techniques, the enclosures in the structures began to play an important role in structural behavior under seismic forces. Then, with the introduction of reinforced masonry, the thickness of the walls decreased dramatically and a rational design method for walls to resist dynamic lateral loads from wind and earthquake came into existence in the 20th century.

Reinforced masonry structures are one of the most common building types for low rise construction worldwide. Reinforced masonry structures consist of concrete masonry, joined by mortar, with reinforcing steel bars and wires in fully grouted cells meeting the appropriate requirements for design and construction. Moreover, various earthquake reconnaissance reports have suggested that reinforced masonry structures perform well in earthquakes provided proper seismic detailing has been incorporated into their design.

1.2 Seismic Risk Analysis

Seismic risk is important because it can often provide insight into the seismic vulnerability of a structure. Knowing the seismic risk for a structure can allow for proper budgetary planning, raise public awareness, help with assessment and allocation of the necessary

manpower for mitigation and disaster management operations, educate the public and professionals on preparedness and mitigation, prioritize retrofit applications, perform damage and loss estimations, and make good retrofit decisions for civil structures [EERI, 1997]. The components that define seismic risk analysis and loss estimation are (1) Hazard Analysis; (2) Local Site effects; (3) Exposure Information; (4) Vulnerability Analysis (Coburn, et al., 1994;; CSSC, 1999; Chandler and Nelson, 2001; Bendimerad, 2001).

The hazard analysis consists of the process of quantitatively estimating the ground motion at a site or region of interest based on the characteristics of surrounding seismic sources. The basic methodology of this analysis is comprised of source modeling, wave attenuation and local ground amplification. The hazard analysis is either a curve showing the exceedance probabilities of various ground motions at a site, or a hazard map that shows the estimated magnitude distribution of ground motions having a specific exceedance probability over a specified time period for a region.

Local geologic and soil conditions significantly influence ground motion characteristics, such as magnitude, frequency content and duration [Kramer, 1996, Marcellini et al., 2001]. Local site effects are essential for determining the ground motion parameters as well as the potential of liquefaction and ground failure. For this reason local site conditions are often considered in the development of a site-specific response spectrum in order to be used in the structural analysis and design.

Vulnerability analysis reveals the damageability of a structure(s) under varying ground motion intensities. Vulnerability can be defined as the sensitivity of the exposure to seismic hazard(s). The vulnerability of an element is usually expressed as a percent loss for a given

seismic hazard severity (intensity) level [Coburn et al., 1994]. Vulnerability of structures to ground motion effects is often expressed in terms of fragility curves or damage functions that take into account the uncertainties in the seismic demand and structures capacity.

1.3 Fragility Analysis and its Graphical Representation

A fragility analysis is an effective tool for risk assessment and vulnerability of structural systems. The fragility curve, which is developed from the structure capacity or behavior model and a suite of ground motions, is a graphical representation of the seismic vulnerability of a structure. Early forms of fragility curves were developed as a function of qualitative ground motion intensities based largely on expert opinion. Recent developments in nonlinear structural analysis have enabled development of fragility curves using numerical models calibrated to experimental data, and are represented as a function of earthquake intensity.

Fragility curves provide a graphical representation of exceeding a drift or damage state as a function of one or more seismic intensity measures (IM). An IM is the reference ground motion parameter against which the probability of exceedance of a given limit state is plotted.

IMs are generally correlated well with the severity of ground shakings with the most common IMs for use in building loss assessment being:

- Spectral acceleration, Sa
- Spectral displacement, Sd
- Peak Ground Acceleration, PGA
- Peak Ground Velocity, PGV

In the current study the Sa is selected as the intensity measure.

The performance levels of a building can be defined through damage thresholds called limit states. These limit states define the threshold between different damage conditions, whereas the damage state defines the damage conditions themselves. The damage states of structures are often based on peak inter-story drift ratio the structure experiences, since this is known to correlate well with certain damage levels. These damage levels are typically then correlated with a performance level such as immediate occupancy, life safety or collapse prevention [ASCE 41, 2006].

Damage Probability Matrices (DPM) consist of obtaining a damage level j , due to a ground of motion of intensity i , $P[D=j/i]$. The concept of a DPM is that a given structural typology will have the same probability of being in a given damage state for a given earthquake intensity. The Vulnerability Index Method [Benedetti and Petrini, 1984] expresses the relationship between the seismic action and the response that is established through a “vulnerability index” [Calvi et al. 2006], and is known as an indirect method. This method uses a field survey form to collect information on the important parameters of the structure which could influence its vulnerability. Another method is a Continuous Vulnerability Functions that are based directly on the damage of buildings from past earthquakes. Some of the empirical vulnerability functions that had been proposed, generally with normal or log-normal distributions, are related to the spectral acceleration or spectral displacement at the fundamental (elastic) period of the building.

The Expert opinion-based fragility curves depend on the judgment and knowledge of the experts. This method is not affected by the limitations regarding the quantity and quality of structural damage data and statistics. It is not an accurate method, because the results depend to the individual expertise of the experts consulted, but it is often one of the only methods available

following an earthquake. These experts are asked to provide an estimate of the probability of damage for different types of structures and typically several levels of ground shaking are available from recordings and, at times, utilize interpolation.

The Analytical Methods tend to feature more detailed and transparent vulnerability assessment algorithms with direct physical meaning, that allow detailed sensitivity studies to be undertaken, and cater to straightforward calibration for various characteristics of building type and hazard. Analytical fragility curves are constructed starting from the statistical response or damage distributions that are simulated from analyses of nonlinear structural models under increasing earthquake intensity.

A type of fragility known as hybrid fragility is based on the combination of observation and numerical analysis for damage prediction. Usually, the main goal is to compensate for a lack of observed data, deficiencies of structural models, and subjectivity in expert opinion data.

Construction of fragility curves provides the key element in the estimation of the probability of various damage states in buildings as a function of seismic intensity. The fragility curves are often generated assuming the demands of the structure follow a lognormal distribution. In earthquake engineering, fragility curves derived from robust nonlinear modeling of reinforced masonry structures are somewhat scarce. Thus, in this thesis, existing data from reversed cyclic testing of masonry walls [Klingner et al., 2010], was used to calibrate nonlinear hysteretic models, perform nonlinear time history analysis, and generate fragility curves for reinforced masonry walls. A nonlinear numerical model was used [Pei and van de Lindt, 2008] to model a reinforced masonry building and subject it to a suite of earthquakes from which fragilities that account for both in-plane and out-of-plane seismic response are developed.

Chapter 2: Data and Modeling Fit

2.1 Network for Earthquake Engineering Simulation (NEES) Data for Masonry

2.1.1 Background and Scope

The US National Science Foundation (NSF) sponsored a research project entitled “Performance-Based Design of Masonry” [Klingner et al. 2010] focusing on four specific areas: (1) experimental research, (2) analytical research, (3) education and (4) development of design recommendations for code implementation. The project focused on the research of reinforced concrete masonry construction with clay masonry veneer, examining all the regulations of the family of applicable codes.

2.1.2 Existing Data on Reinforced Concrete Masonry Specimens with Clay Masonry Veneer

The seismic performance of reinforced concrete masonry walls with clay masonry veneer was experimentally evaluated by Klingner et al. [2010]. This consisted of testing twelve concrete masonry walls assemblies that were quasi-statically and dynamically tested at The University of Texas at Austin and at the NEES outdoor shake table at the University of California at San Diego. Six were tested out-of-plane and the six were tested in-plane. Table 2.1 summarizes the configuration of each wall specimen.

Table 2.1 Overview of Wall Specimens Configuration

Specimens	Loading	Dimensions	Reinforcement	Connectors	Mortar
UT CMU1	Out of Plane Quasi-static	8-ft (2.44-m) wide by 8-ft (2.44-m) high	five No. 4 bars vertically and three No. 4 bars horizontally	double eye-and-pintle	S cement lime
UT CMU2				tri-wire	S cement lime
UT CMU2 MC				tri-wire	S masonry cement
UT CMU 3	In-plane Quasi-static	4-ft (1.22-m) wide by 8-ft (2.44-m) high	two No. 4 bars vertically and three No. 4 bars horizontally	double eye-and-pintle	cement-lime
UT CMU 4				tri-wire	cement-lime
UT CMU 4 MC				tri-wire	masonry cement
UCSD CMU 1	Out-of-Plane Table-Shaking	8-ft (2.44-m) wide 8-ft (2.44-m) high	five No. 4 bars vertically and three No. 4 bars horizontally	double eye-and-pintle	cement-lime
UCSD CMU 2				tri-wire	cement-lime
UCSD CMU 2 MC				tri-wire	masonry cement
UCSD CMU 3	In-Plane Table-Shaking	4-ft (1.22 m) wide 8-ft (2.44 m) high	two No. 4 bars vertically and three No. 4 bars horizontally	double eye- and-pintle	cement-lime
UCSD CMU 4				tri-wire	cement-lime
UCSD CMU 4 MC				tri-wire	masonry cement

Then, a full-scale, one-story masonry building specimen was designed by University of Texas at Austin researchers and tested on the NEES outdoor shake table at the University of California at San Diego.

One of the objectives of the project by Klingner et al. [2010] was to examine the flexural and base sliding behavior for in-plane concrete masonry walls using the quasi-static testing; the behavior of the veneer connectors, and the rocking and base sliding behavior of the in-plane veneer, using the dynamic testing.

The CMU wall specimens and their veneers were loaded out-of-plane, for both quasi-static and dynamic testing, and the report focus in their study was on inelastic behavior, specifically determining that the maximum capacity of the quasi-static, and confirming that the out-of-plane CMU wall specimens was always governed by the connectors. In those tests the

load was applied directly to the clay masonry veneer, however under real earthquake excitations because of the additional inertia forces induced in the CMU walls, the capacity could be governed either by the connectors or by the CMU wall itself. In the dynamic testing, the out of plane veneer acts as attached mass to the CMU wall, so when the out-of-plane connectors fails, the veneer generally collapses [Klingner et al. 2010].

For the analytical phase of that research, nonlinear numerical models were developed using OPENSEES. The models capture the essential behavior of the in-plane wall segments, out-of-plane wall segments and the CMU building specimen as a whole. Their analysis looked for flexural hinging or sliding at the base of the in-plane CMU walls, rocking and sliding of the in-plane veneer along with the connectors, flexural hinging at the base and at around the mid-height of the out-of-plane CMU walls, and tensile yielding and compressive buckling of the out of plane connectors.

The Klingner et al. [2010] report concludes that the clay veneer has a negligible effect on overall response in the elastic range, but a significant effect in the inelastic range. The investigators recommended that the CMU building specimen have continuity at the veneer's corners because this can provide a reduction in the sliding of the in-plane veneer. The researchers point out that the out-of plane veneer is more affected by differences in connectors' axial strength, than by differences in their axial stiffness.

The in-plane CMU walls responded as rigid bodies in the study by Klingner et al. [2010], essentially rotating and sliding at their bases. Their behavior was governed by flexural hinging, base sliding or a combination of both. Likewise, in the CMU building specimen and the shake-table CMU wall specimens, the in-plane veneer and its connectors performed well under

repeated earthquakes without falling off the in-plane CMU showing that the in-plane veneer rocked or slid, and the connectors yielded. The study also showed that the sliding resistance of the veneer depends on two factors, namely the coefficient of friction between the veneer and the shelf angle on which the veneer was laid, and on the in-plane resistance of the connectors which affected the rocking resistance.

Another highlight shows that the response of the out-of-plane CMU walls with clay masonry veneer is governed by the ground motion at the base and by the response of the roof diaphragm. With high levels of shaking, the CMU walls developed flexural hinges at the base and at mid-height. When the roof diaphragm was laterally flexible enough, flexural hinges were formed only at the base. Because of the flexural stiffness of the veneer is small in comparison with the flexural stiffness of the CMU walls, they conclude that the veneer acts as a mass only.

They also confirmed that the seismic response of CMU buildings is controlled by the response of the in-plane CMU walls. The out-of-plane veneer and the in-plane veneer showed a minor cracking without significant damage to their connectors. Moreover the in-plane veneer experienced some rocking and sliding.

2.1.3 Database used for Thesis.

During the experimental research [Klingner et al. 2010], the behavior of twelve reinforced masonry walls were analyzed under quasi-static and dynamic loading. Six reinforced concrete masonry wall specimens were tested quasi-statically and the other six specimens were tested dynamically, both of them under out-of-plane and in-plane loading. For the quasi-static loading, three specimens were tested under the out-of-plane loading (Figure 2.1) and the other three specimens were tested under in-plane loading (Figure 2.2). The out-of-plane loading was

based on target load levels until the maximum load capacity was reached, after which it was based on target displacement levels at the mid-height of the masonry veneer. The loading protocol consisted of a series of three reversed cycles to a maximum load capacity that was increased monotonically in increments of 4.0 kips (17.8 kN), corresponding to increments of 62.5 psf (2.99 kPa). After the specimen reached its maximum load capacity, a series of three reversed cycles were continued to monotonically increasing maximum displacement levels at the mid-height of the clay masonry veneer equal to 1.5, 2.0, 3.0 and 5.0 times the displacement at maximum load capacity. The in-plane loading was based on target load levels until flexural cracking occurred, after which it was based on target displacement levels. The loading protocol consisted of three stages; the first stage was three reversed cycles of a load to flexural cracking; the second stage was series of three reversed cycles to target displacements, increased monotonically in increments of 0.25 in (6.4 mm) until the specimen reached its maximum load capacity and the third stage consist of a series of three reversed cycles to monotonically increasing maximum displacement levels equal to 1.5, 2.0, 3.0 and 5.0 times the displacement at maximum load capacity.

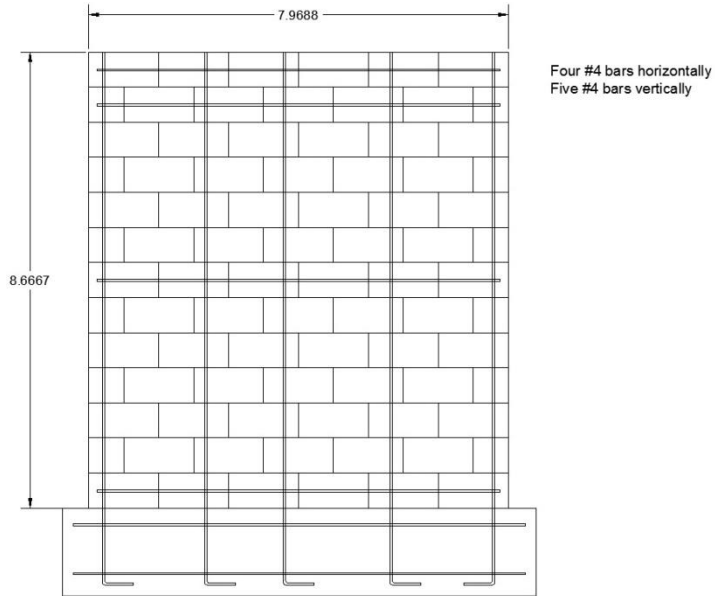


Figure 2.1 Out – of – Plane CMU Wall Specimen tested by Klingner et al. [2010]

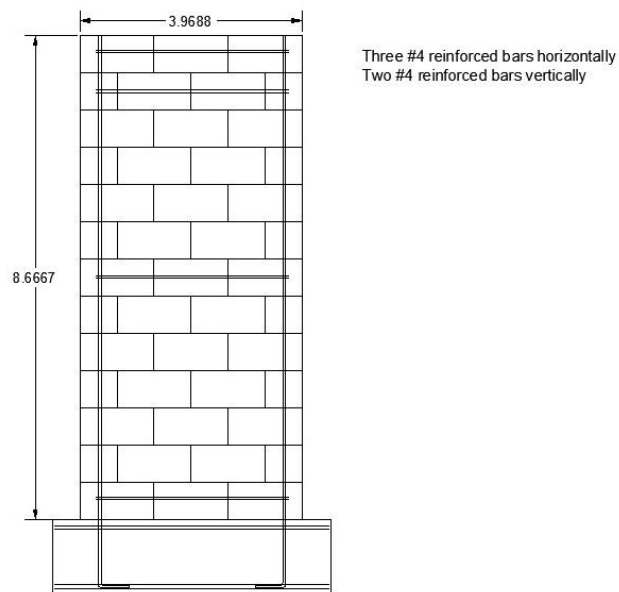


Figure 2.2 In-Plane CMU Wall Specimen tested by Klingner et al. [2010]

For the dynamic testing of the CMU wall specimens, three specimens were tested under the out-of-plane loading and other three specimens were tested under the in-plane loading. Two ground motion records, obtained from the Center for Engineering Strong Motion Data, which belong to the 1994 Northridge (California) Earthquake, were used: the Sylmar (Figure 2.3) with

a total duration of 40 seconds and the Tarzana (Figure 2.4) with a total duration of 60 seconds. Each CMU wall specimen was first subjected to a sequence of Sylmar ground motion histories scaled to different levels, and then to scaled Tarzana ground motions. The typical damping ratio of 5% was used for the calculation of the spectral values.

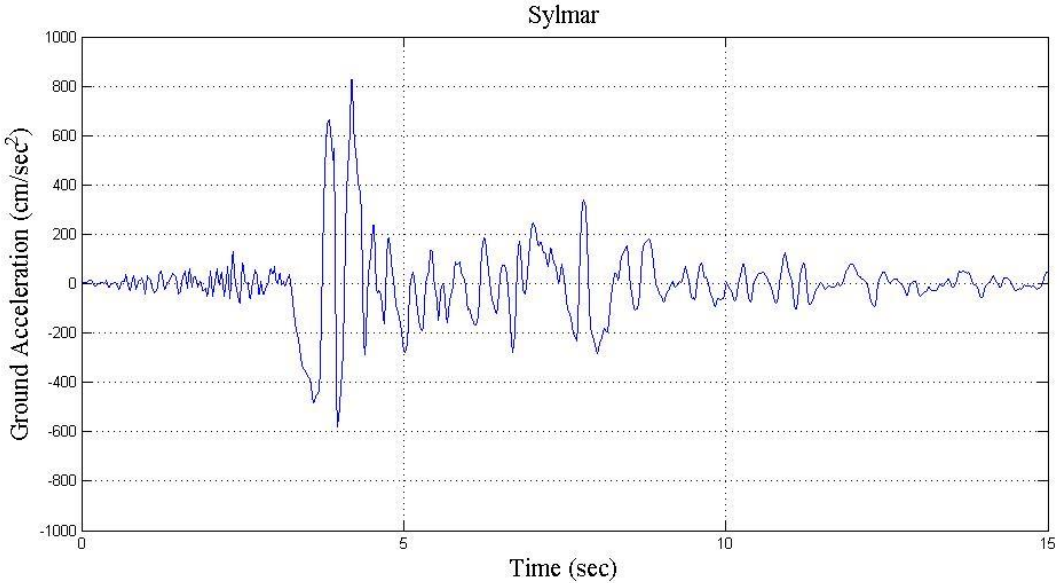


Figure 2.3 Sylmar Record

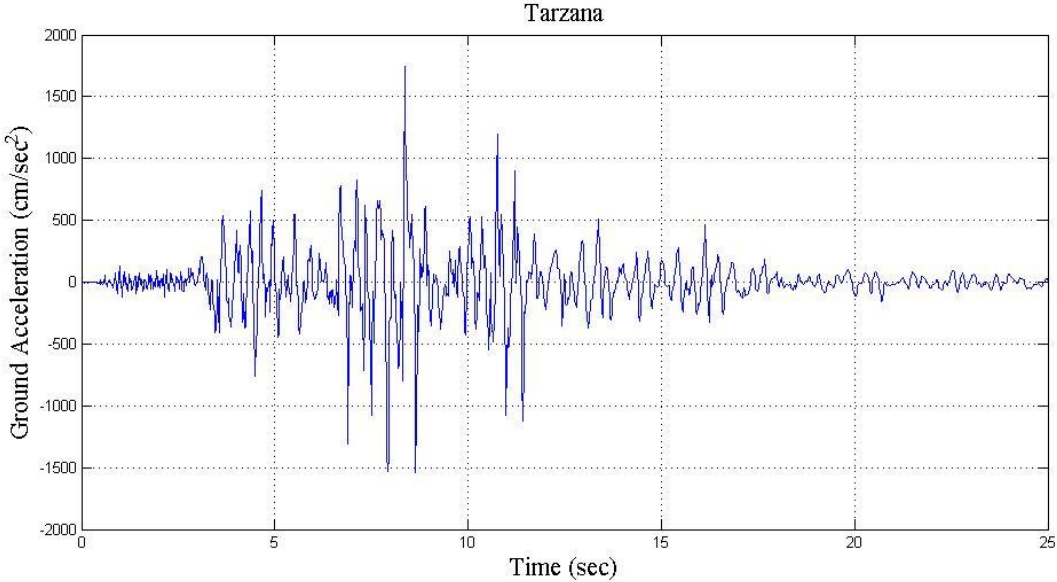


Figure 2.4 Tarzana Record

The main purpose of the dynamic testing was to compare the results of that testing with the quasi-static results and provide experimental data to develop and calibrate analytical models for that out of plane and in plane response.

In this thesis the data from tests executed at the University of Texas in Austin on CMU wall specimens were quasi-statically under out-of-plane and in-plane loading is utilized. Specifically, the focus is on the loading and displacements of the CMU walls, when the loading is applied at the top of the CMU wall specimens.

2.2 Modeling Approach

2.2.1 Hysteretic Behavior

Analytical modeling of an inelastic structure under dynamic loading ideally requires a force-displacement relation, or hysteresis model, that can reproduce the true behavior of the structure at all displacement levels including strength and stiffness degradation as it cycles through displacements during an earthquake. Different models have been developed to model lateral load displacement relationships. For example, Wakabayashi and Nakamura (1984) combined arch and truss mechanisms in order to predict lateral load-displacement skeleton curves to model the shear failure of reinforced masonry walls. Tassios (1984) proposed a combination of dowel pullout and friction mechanisms to model the skeleton curve as well as hysteretic behavior. Bernardini et al. (1984), however, proposed a global implicit dimensionless analytical hysteretic model on the basis of experimental results of cyclic tests of reinforced masonry walls. Tanrikulu et al. (1992) modeled the hysteretic behavior of plain masonry walls with shear failures using parameter functions, and determined their loading and unloading characteristics by experiments.

The basic backbone curve of hysteresis loops can be accurately determined from monotonic experiments. However, data regarding the hysteretic behavior of the walls, such as strength and stiffness degradation and deterioration and energy dissipation capacity, requires reversed-cyclic testing of masonry wall.

2.2.2 Hysteretic Modeling

A recent model for seismic structural analysis of shear walls under general cyclic loading which predicts the load-displacement response and energy dissipation characteristics under quasi-static cyclic loading developed during the CUREE – Caltech Woodframe Project was used in this thesis [Folz and Filiatraut, 2001]. This model is the ten-parameter hysteretic model used in the Cyclic Analysis of Wood Shear Walls (CASHEW) program [Folz and Filiatraut 2000, 2001] and was based on Stewart's model (1987) where he developed hysteretic models for sheathing to wood connections using piecewise linear curves to trace the loading and unloading paths forming an envelope curve. This model was originally proposed by Foschi (1977) in which six physically identifiable parameters must be fit to experimental data: F_0 , K_0 , r_1 , r_2 , δ_u , and δ_f where δ_u is the ultimate displacement corresponding to F_u (ultimate loading) and δ_f is the displacement corresponding to the failure.

Unloading off this curve is assumed elastic along path 3, followed by a pinched response along path 4, which passes through the zero-displacement intercept with slope $r_4 K_0$. Continued reloading follows path 1 with degrading stiffness K_p as given by

$$K_p = K_0 (\delta_0 / \delta_{max})^\alpha \quad (4)$$

With $\delta_0 = (F_0 / K_0)$; and α = hysteretic model parameter that determines the degree of stiffness degradation. K_p is function of the previous loading history through the last unloading displacement δ_{un} off the envelope curve so that

$$\delta_{max} = \beta \delta_{un} \quad (5)$$

Where β = hysteretic model parameter. The parameters β and α are obtained by fitting the model to connection test data.

The ability of a hysteretic model to accurately predict the dynamic response of shear walls is essential for further development and ultimate implementation of a performance-based-seismic design (PBSD) methodology Pang et al. (2010).

The load-displacement curves obtained for quasi-static out-of-plane and in-plane experimental testing by Klingner et al. (2010), are shown in Figure 2.6 for the Masonry Specimen UT CMU1 (Out-of-Plane) and in Figure 2.7 for the Masonry Specimen UT CMU3 (In-Plane), respectively.

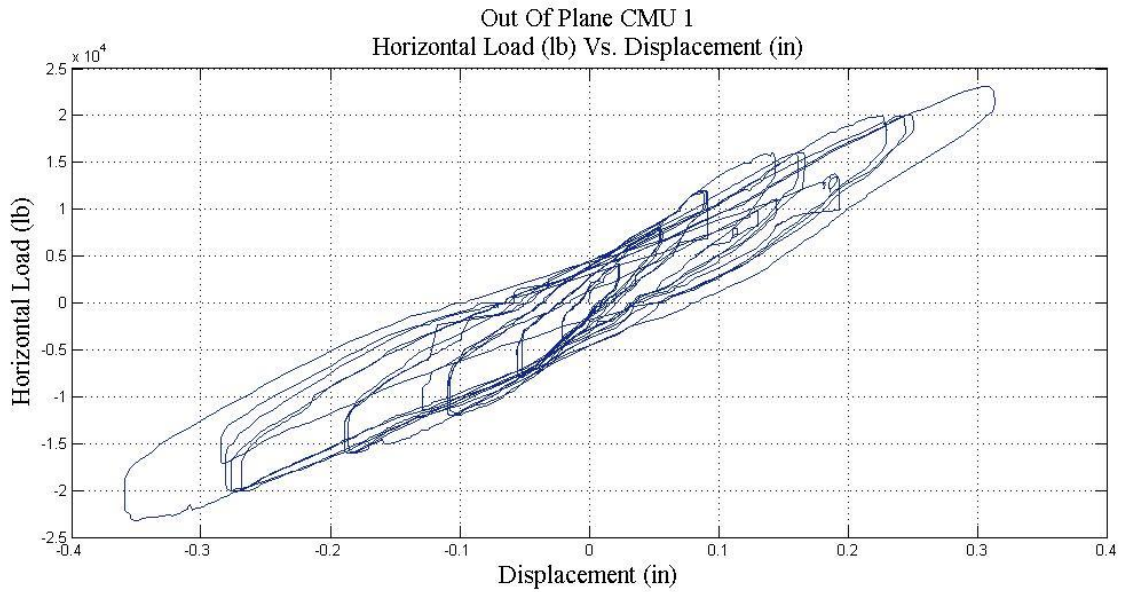


Figure 2.6 Load Versus Displacement at the Top of a CMU Out-of-Plane Wall

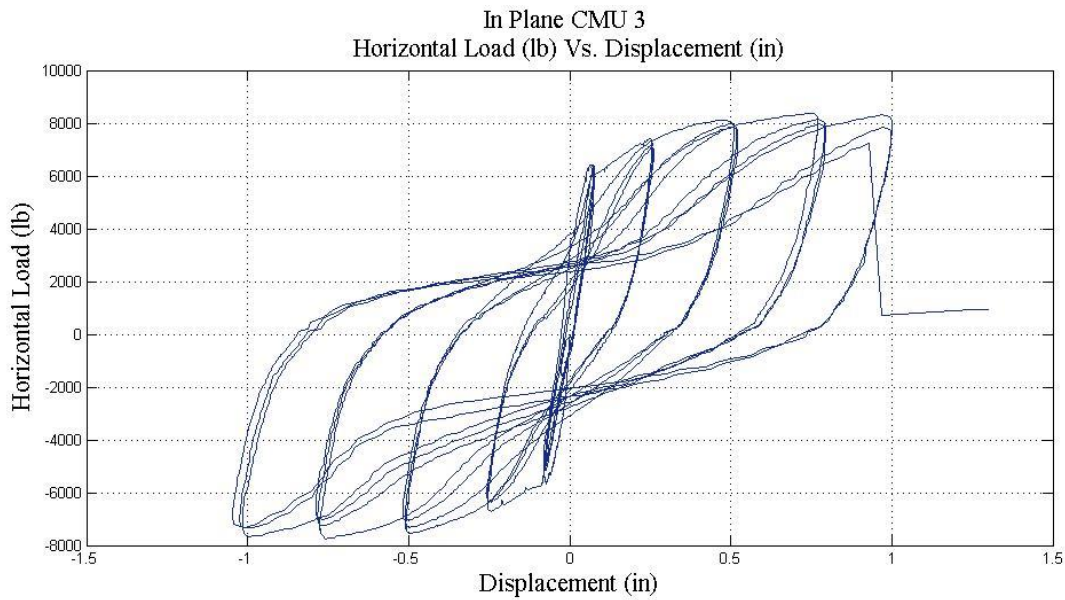


Figure 2.7 Load Versus Displacement at the Top of a CMU In-Plane Wall

2.3 Modeling of Masonry Walls

The software SAPWood Version 2.0 which was developed by Pei and van de Lindt (2009) as part of the NEESWood Project was selected in this study for modeling the behavior of

the low rise reinforced concrete masonry walls. This analysis program is based on the Seismic Analysis of Woodframe Structures (SAWS) [Folz and Filiatraut, 2002a; 2002b]. The software performs nonlinear time history analysis (NLTHA) for woodframe structures. SAPWood Version 2.0 includes non-linear spring elements with a variety of possible nonlinear behaviors. These non-linear spring elements can be used to develop nonlinear models for a low rise reinforced concrete masonry building as illustrated in Figure 2.8.

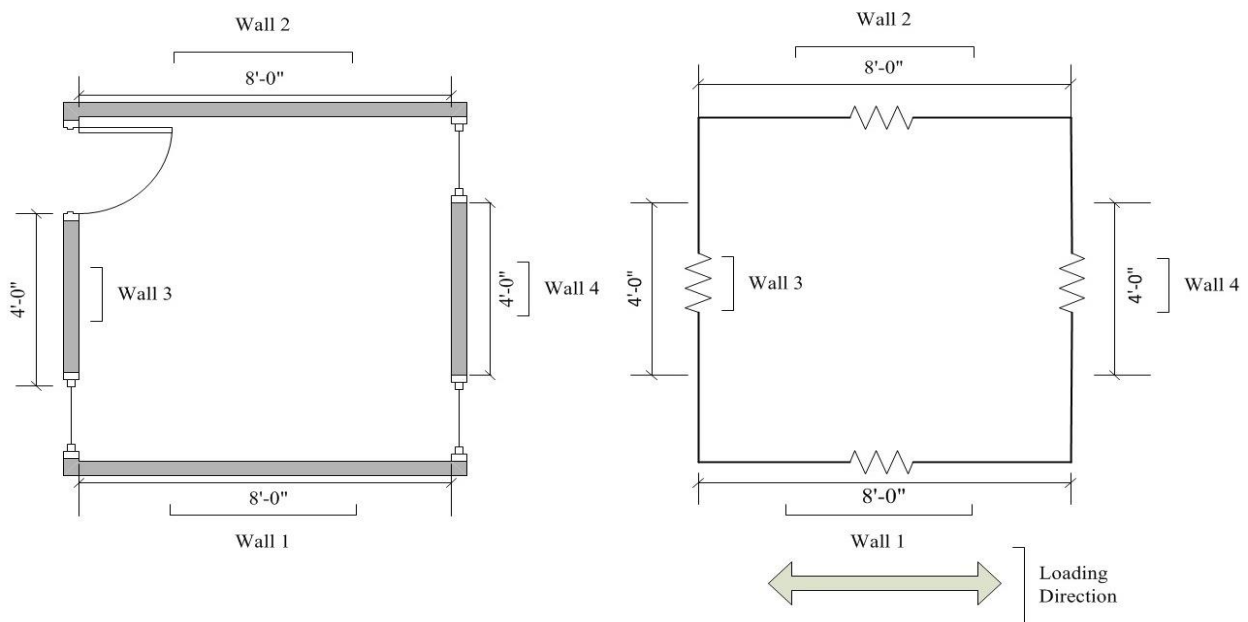


Figure 2.8 Composite Spring Model of a CMU Building

There are four spring models included in the SAPWood package; however in this project the most appropriate is the SAWS-type ten-parameter hysteretic model that will allow modeling of the lateral load-resistance behavior of the shear wall and out-of-plane components. The ten parameters (Table 2.2) were obtained from the fit of the ten-parameter model to the wall hysteresis data from the cyclic wall tests [Klingner et al. 2010] conducted at the University of Texas at Austin as shown in Figure 2.9 and Figure 2.10.

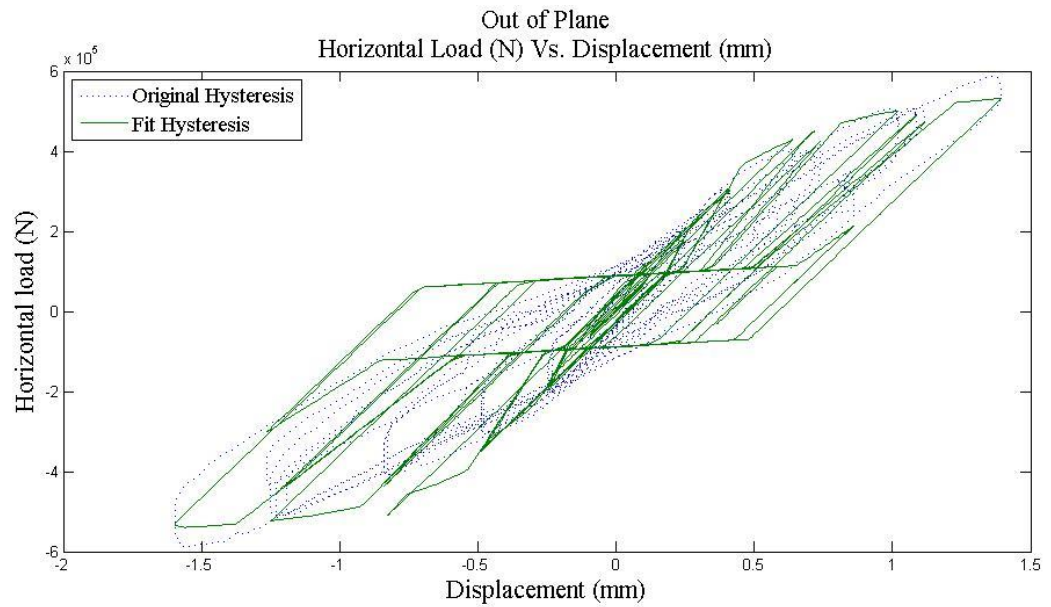


Figure 2.9 Fit Hysteresis of an Out-of-Plane CMU Wall

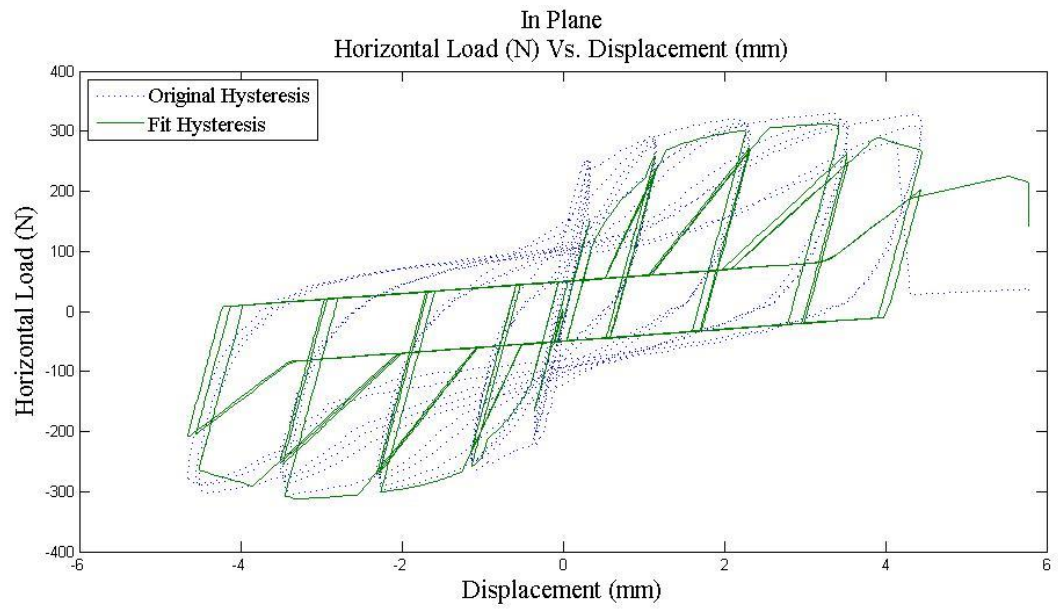


Figure 2.10 Fit Hysteresis of an In-Plane CMU Wall

Table 2.2 Fitted Hysteretic Parameters

Parameters	Out-of-Plane Wall	In-Plane Wall
Ko	2.31E+05	5.62E+04
F0	2.09E+04	7.55E+03
F1	3.48E+03	1.26E+03
r1	1.00E-02	1.00E-02
r2	-9.00E-02	-8.00E-02
r3	5.00E-01	1.00E+00
r4	3.00E-02	2.00E-02
Xu	3.51E-01	7.46E-01
Alpha	7.50E-01	7.50E-01
Beta	1.10E+00	1.10E+00

SAPWood 2.0 was used to model a low rise reinforced concrete masonry building using in-plane and out-of-plane hysteretic models for each wall. A suite of twenty two earthquakes was used for nonlinear time history analysis. These twenty-two acceleration records, each a historical earthquake, are listed in Table 2.3.

Table 2.3 Far-Field Earthquake Records – FEMA P695

Earthquake			Record Station	
Magnitude	Year	Name	Name	Owner
			Beverly Hills - 14145	
6.7	1994	Northridge	Mulhol	USC
			Canyon Country-W Lost	
6.7	1994	Northridge	Cany	USC
7.1	1999	Duzce, Turkey	Bolu	ERD
7.1	1999	Hector Mine	Hector	SCSN
6.5	1979	Imperial Valley	Delta	UNAMUCSD
6.5	1979	Imperial Valley	El Centro Array #11	USGS
6.9	1995	Kobe, Japan	Nishi-Akashi	CUE
6.9	1995	Kobe, Japan	Shin-Osaka	CUE
7.5	1999	Kocaeli, Turkey	Dusze	ERD
7.5	1999	Kocaeli, Turkey	Arcelik	KOERI
7.3	1992	Landers	Yermo Fire Station	CDMG
7.3	1992	Landers	Coolwater	SCE
6.9	1989	Loma Prieta	Capitola	CDMG
6.9	1989	Loma Prieta	Gilroy Array #3	C
7.4	1990	Manjil, Iran	Abbar	BHRC
6.5	1987	Superstition Hills	El Centro Imp. Co. Cent	CDMG
6.5	1987	Superstition Hills	Poe Road (temp)	USGS
7	1992	Cape Mendocino	Rio Dell Overpass - FF	CDMG
7.6	1999	Chi-Chi, Taiwan	CHY101	CWB
7.6	1999	Chi-Chi, Taiwan	TCU045	CWB
6.6	1971	San Fernando	LA - Hollywood Stor FF	CDMG
6.5	1976	Friuli, Italia	Tolmezzo	---

2.4 Fragility Curves

A fragility is defined as a conditional probability which provides the probability of a structure reaching or exceeding a specified limit state under a given earthquake intensity level (i.e., spectral acceleration at the building fundamental period in the case of seismic hazards). As such, fragility curves are a measure of performance in probabilistic terms that can be developed either for a specific system or component or for a group of components. The so-called fragility

curves can be used in an “uncoupled analysis to evaluate failure probabilities by convolving with a probabilistic description of the demand or used to compare different seismic rehabilitation techniques in order to optimize the seismic design of a structure” [Rosowsky and Ellingwood 2002].

There are two main approaches for generating fragility curves. One is based on damage data obtained from field observations after an earthquake or from experiments and the other approach utilizes numerical analysis of the structure, either through non-linear time history analysis or a simplified methods. These were summarized earlier in the introduction of this thesis.

The fragility of a structure is often model by a lognormal distribution given by

$$F_R(S_a) = \Phi \frac{\ln(S_a) - m_R}{\varepsilon_R} \quad (6)$$

Where $\Phi(\cdot)$ is the standard normal cumulative distribution function; m_R is the logarithmic median capacity; and ε_R is the logarithmic standard deviation capacity.

Then,

$$P[D \geq d_{s_i} | S_{a_n}] \quad (7)$$

Where $P[D \geq d_{s_i} | S_{a_n}]$ is the probability of the structural response exceeding the i-th limit state expressed as a threshold, d_{s_i} and D is a damage measure.

Chapter 3: Modeling of a Low-Rise Reinforced Masonry Building

Reinforced masonry structures are usually “box” systems, in which shear wall panels resist the vertical as well as lateral loads [Shing et al., 1990]. The structural behavior of masonry can be very complex even under static loading. A typical reinforced masonry building is the one that is a small, low-rise (one or two-story in height) structure. For our research, a one story building has been designed to represent an illustrative reinforced masonry building. The detailed dimensions for each wall and a plan view of the models are shown in table 3.1 and figure 3.1 and figure 3.2.

Table 3.1 Overview of Wall Specimens Specifications

Specimen	Model 1 Dimensions	Loading Direction
Wall 1 and Wall 2	8 ft wide by 8 ft high	In – Plane
Wall 3 and Wall 4	4 ft wide by 8 ft high	Out – Of – Plane
Wall 5 and Wall 6	4 ft wide by 8 ft high	In – Plane

Specimen	Model 2 Dimensions	Loading Direction
Wall 1 and Wall 2	8 ft wide by 8 ft high	In – Plane
Wall 3 and Wall 4	4 ft wide by 8 ft high	Out – Of – Plane
Wall 5 and Wall 6	4 ft wide by 8 ft high	Out – Of – Plane

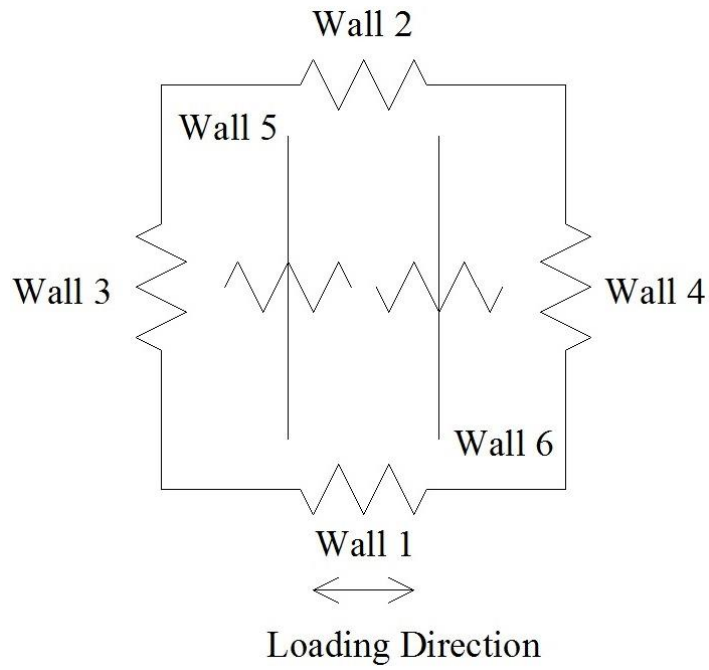


Figure 3.1 Spring Model of In-Plane Wall

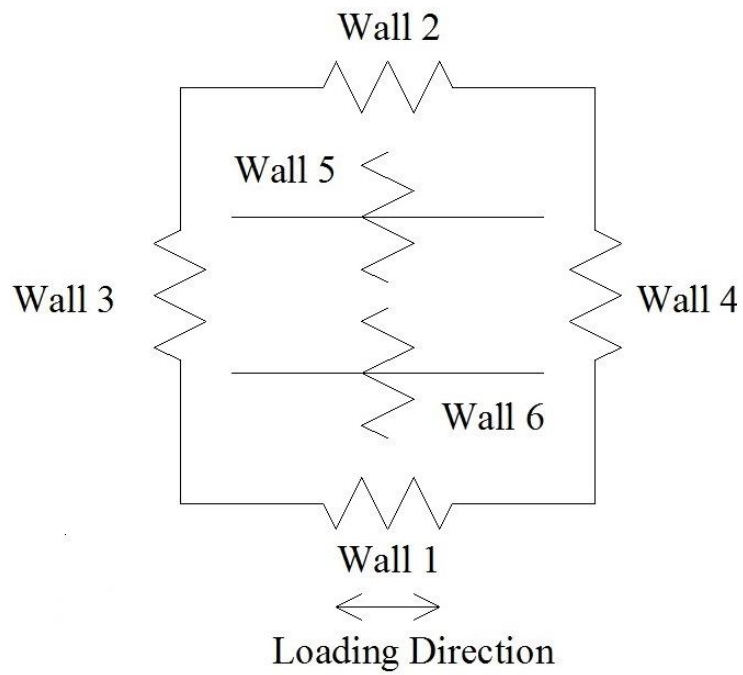


Figure 3.2 Spring Model of Out-of-Plane Wall

Six reinforced masonry walls, referred to Wall 1, Wall 2, Wall 3, Wall 4, Wall 5 and Wall 6 define the small building. The building is 8 feet by 8 feet with a story height of 8 feet. Walls 1 – 4 are shear walls and wall 5 and 6 are transverse representation of walls 3 and 4, respectively. All the material properties were obtained from the experimental study by Klingner et al. [2010].

In reality, an earthquake is a three-dimensional excitation to the building. Many buildings have irregular layouts that can result in a building structure that behaves in even a more complex three-dimensional way under seismic loading. Therefore, three dimensional analyses should produce a more accurate description of the behavior of the structure, and this might include torsional responses caused by asymmetry of the distance between the center of rigidity and the center of mass. Nevertheless, the models developed for this study are based in a two-dimensional behavior composed of zero-height shear wall spring elements, assuming that the ground motion excitation is parallel to Wall 1 and Wall 2. This is mainly because the focus is on the later development of fragilities which can be done with a model of any complexity. Therefore, in this thesis a simpler model that will be efficient enough for repetitive dynamic analyses but accurate enough to capture the strength and stiffness degrading hysteretic behavior of the masonry and stiffness of the transverse shear walls is used.

The first model (Figure 3.1) is composed of four zero-height shear spring elements and two zero height out-of-plane spring elements; and the second model (Figure 3.2), is composed of two zero-height shear spring elements and four zero height out-of-plane spring elements. The force-deformation response of each shear wall spring element requires specification of 10 hysteretic parameters. These parameters were obtained using the analysis program SAPWood version 2.0 [Pei and van de Lindt, 2008] and the available test data [Klingner et al., 2010]. These

hysteretic parameters values were adjusted and visually/manually calibrated to represent the test data walls in the test structure.

3.1 Modeling of Out-of-Plane Walls

An out-of-plane wall (Figure 3.3) is a building wall that is perpendicular to the direction of the earthquake input or force generated from initial mass. Its lateral stiffness is significantly lower than that of the in-plane wall [Park et al., 2008]. Out – of - plane failures are generally quite brittle unless significant compressive loads are present. Failure or even collapse of the out-of-plane walls under earthquakes is very likely if the connections between the out-of-plane walls and the diaphragms and/or the in-plane walls are not well constrained. Therefore, the dynamic behavior of out-of-plane walls can be quite complex and difficult to characterize because they can have multiple simultaneous failure modes [Kim and White, 2004]. In this study, an out-of-plane wall is modeled with a single nonlinear spring with bi-linear hysteresis behavior and the stiffness is neglected. Only the mass is considered for the dynamic analysis. Failure is not explicitly modeled.

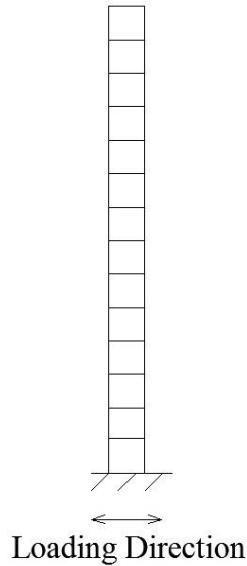


Figure 3.3 Out-of-Plane Concrete Masonry Wall

3.2 Modeling of In-Plane Walls

An in-plane wall (Figure 3.4) is a building wall that has the same direction of the earthquake inputs. Shear wall panels are the major seismic load-resisting elements in reinforced masonry structures. In the in-plane walls, the flexural strength increases with the applied axial stress and the amount of vertical reinforcement present, and shear strength is dominated by diagonal cracking which increases with the amount of vertical and horizontal steel, as well as with the tensile strength of masonry and the applied axial stress [Shing et al., 1990].

To get more accurate results to model the nonlinear behavior of in-plane walls, a simple nonlinear spring model is utilized for this study [Park et al., 2002]. The basic approach to develop a spring model for the in-plane behavior of a reinforced masonry building wall is in which the wall is represented by a nonlinear spring, and the springs are assembled in series and parallel arrangements to match the structural configuration/layout.

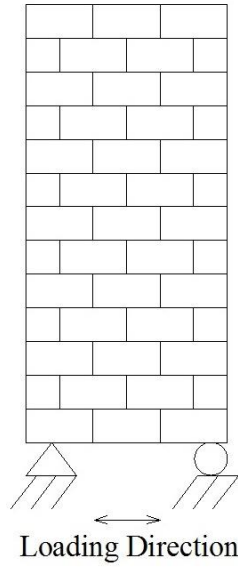


Figure 3.4 In-Plane Concrete Masonry Wall

Although there are not dimensions typical of a regular building they illustrate the use of the nonlinear spring model well. In reality, there would be a “box-like” effect from such a small structure, but it will not be present in this model.

Chapter 4: Fragility Analysis of the low-rise reinforced masonry walls

Under a given ground intensity level S_{a_n} , $P[D \geq d_{s_i}|S_{a_n}]$, where D is a damage measure, is the probability of the structural response exceeding the i-th limit state expressed as a threshold, d_{s_i} . This probability increases, in a direct way, with increasing seismic intensity level. This probability can be calculated if the probability distribution of the structural damage for a given earthquake level is obtained by accounting for stochastic variations of material properties and the variation in the earthquakes themselves.

4.1 Damage Measures

To develop fragility curves, the first step is to define a measure for quantifying the building damage that results from an earthquake. Different researchers have proposed different damage measures. Wong et al. [2001] proposed a damage measure using energy based criteria and Aristizabals [1999] proposed a damage measure using displacement-based criteria such as the maximum roof drift ratio. In the thesis the maximum story drift ratio is used to assess building performance and levels of damage to structural components. The damage or performance levels are then specified as a function of the maximum drift the building sustains during an earthquake. ASCE-41 defines three performance levels for a reinforced masonry structure that are summarized and described in Table 4.1.

Table 4.1 Structural performance levels for reinforced masonry buildings (Excerpted from ASCE 41-06 [2006]).

Structural performance Levels			
Element	Collapse Prevention S – 5	Life Safety S - 3	Immediate Occupancy S - 1
Reinforced Masonry Wall	Crushing; extensive cracking. Damage around openings and at corners. Some fallen units. Drift: 1.5% transient or permanent	Extensive cracking (<1/4”) distributed throughout wall. Some isolated crushing. Drift: 0.6% transient; 0.6% permanent	Minor (<1/8” width) cracking. No out-of-plane offsets. Drift: 0.2% transient; 0.2% permanent

4.2 Ground Motions

For the construction of fragility curves, it was implicitly assumed that there is an equal probability of any one of the records within the selected ground motions suite occurring. The response spectra for the 22 earthquakes [FEMA, 2009] used in this thesis to develop the fragilities are shown in Figure 4.1.

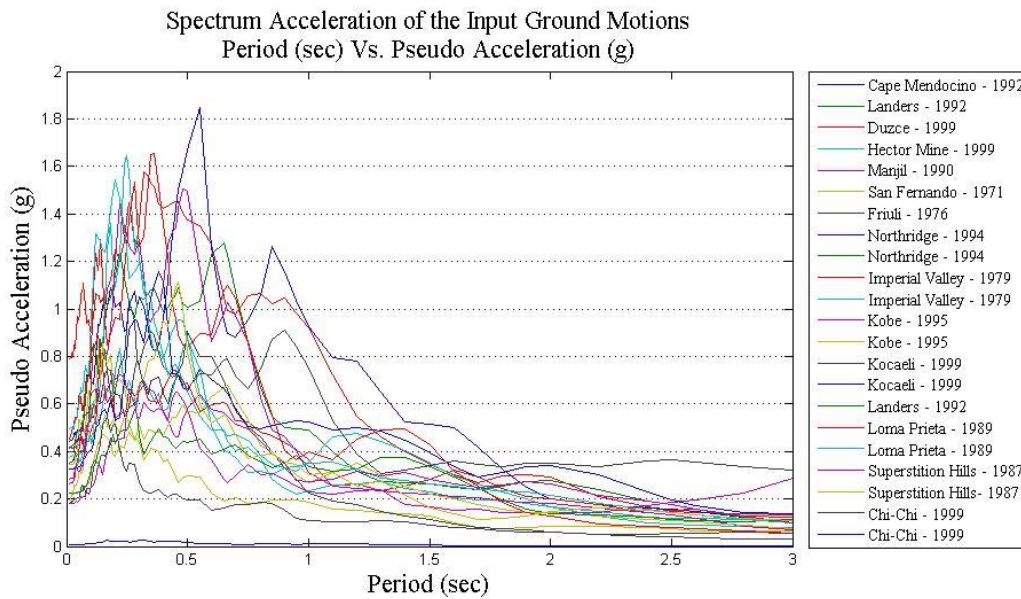


Figure 4.1 Response Spectra for the 22 Earthquakes [FEMA, 2009]

4.3 Construction of Fragility Curves

The SAPWood models representing low-rise reinforced masonry buildings were subjected to the suite of 22 earthquakes for non-linear time history analyses to predict the peak story drifts for each record. As discussed earlier, the ten parameter hysteretic model accounted for the nonlinear behavior of the masonry walls.

Results from the analyses were associated with peak story drift limit states which according to ASCE 41 are correlated with damage, and were then used for the construction of fragility curves. Recall the correlation between performance state and story drifts in reinforced masonry structures were described in the Table 4.1.

The fragility curves presented in this paper are based on force-displacement relationship for walls 5 and 6 obtained from cyclic test results from the two analytical models mentioned before. Figure 4.2 shows the behavior of walls 5 and 6 under in plane loading direction and Figure 4.3 shows the behavior of walls 5 and 6 under out of plane loading direction.

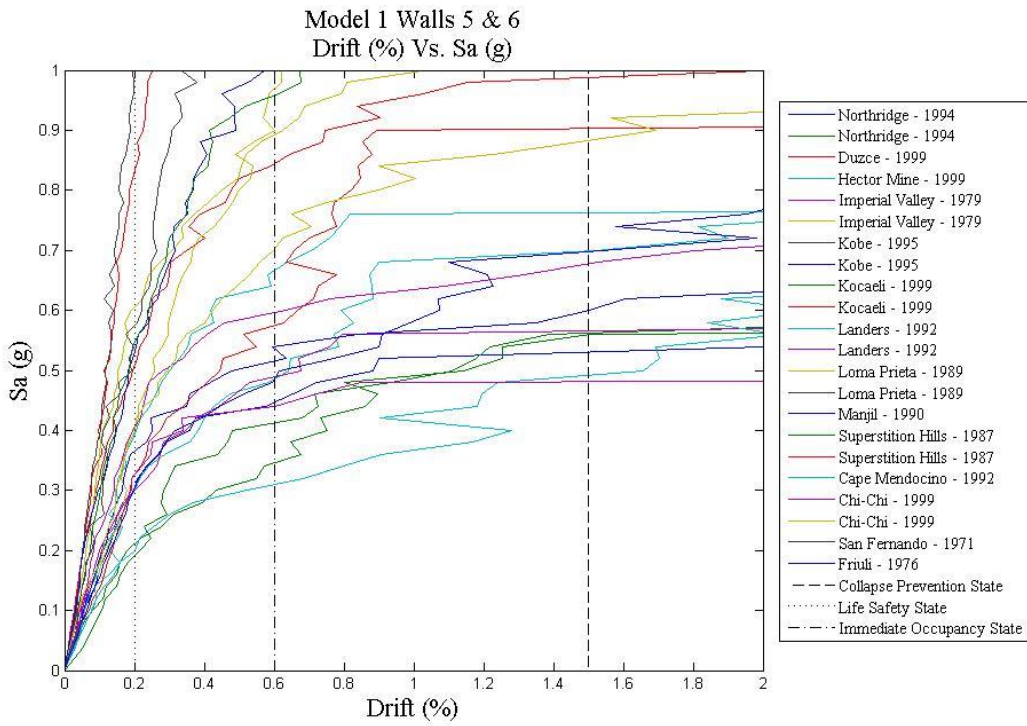


Figure 4.2 Drift Ratio Versus Spectral Acceleration for In-Plane Walls

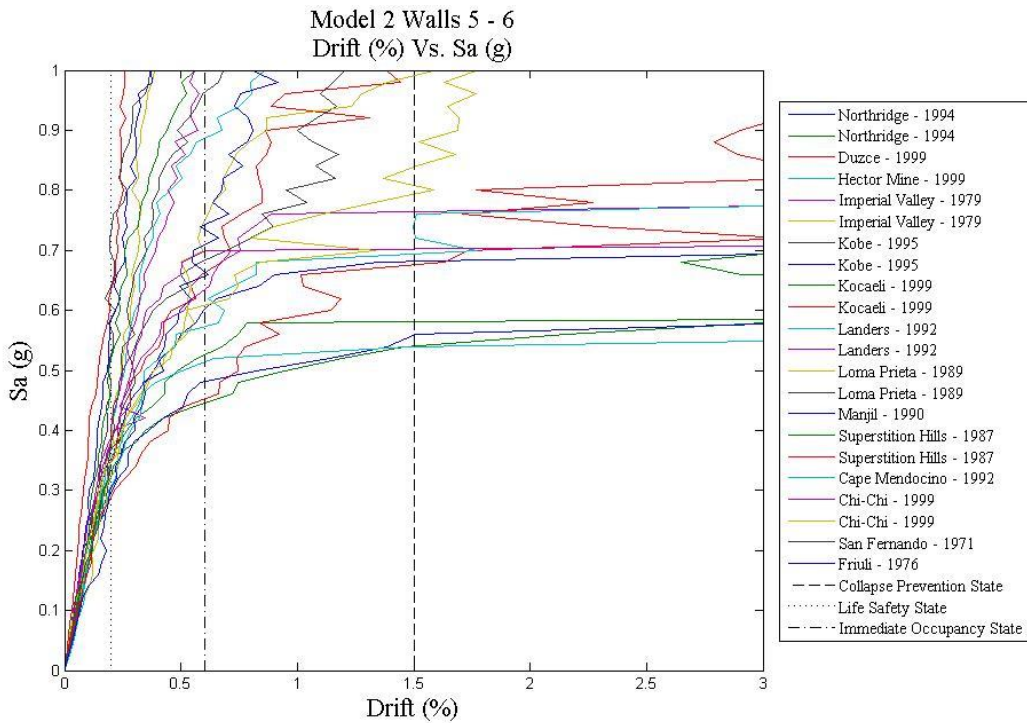


Figure 4.3 Drift Ratio Versus Spectral Acceleration for Out-of-Plane Walls

Fragility curves for the Immediate Occupancy, Life Safety, and Collapse Prevention Limit States are shown below. Figure 4.4, figure 4.5 and figure 4.6 show the fragility curves of walls 5 and 6 under in plane loading direction. Figure 4.7, figure 4.8 and figure 4.9 show the fragility curves of walls 5 and 6 under the out of plane loading direction.

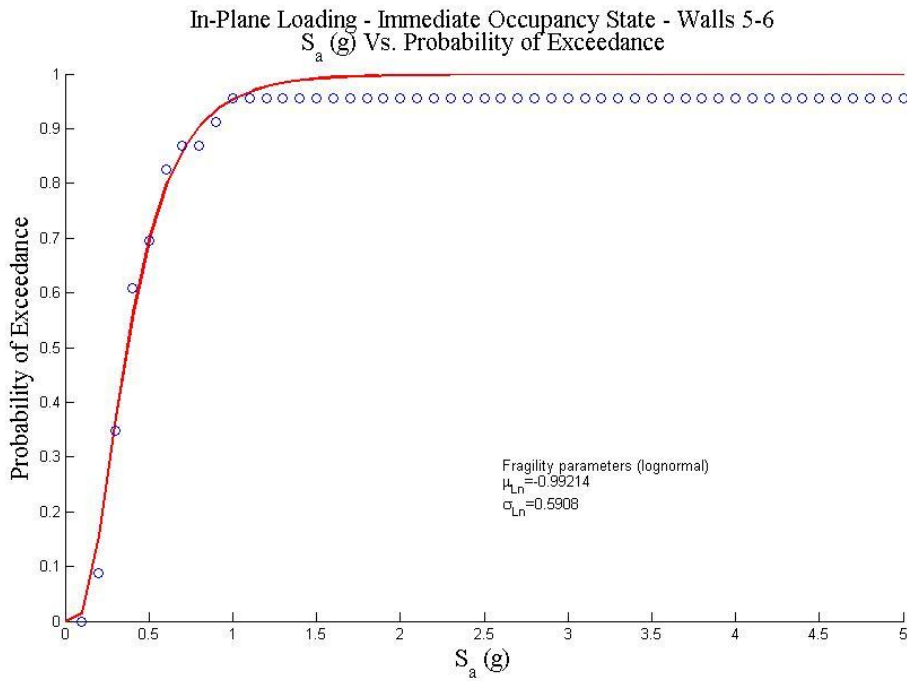


Figure 4.4 Fitted Fragility Curve for In-Plane Walls

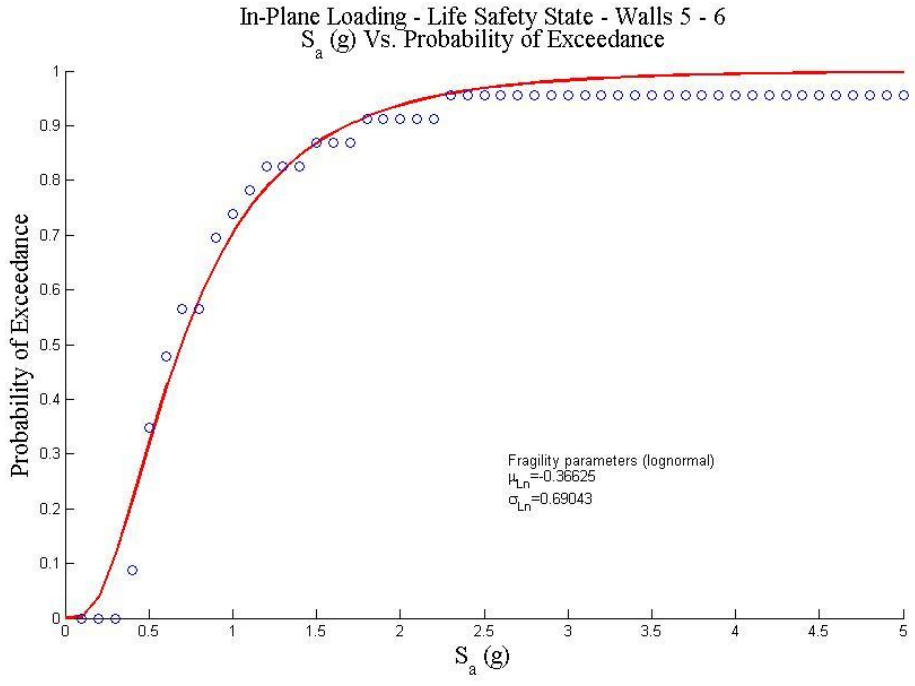


Figure 4.5 Fitted Fragility Curve for In-Plane Walls

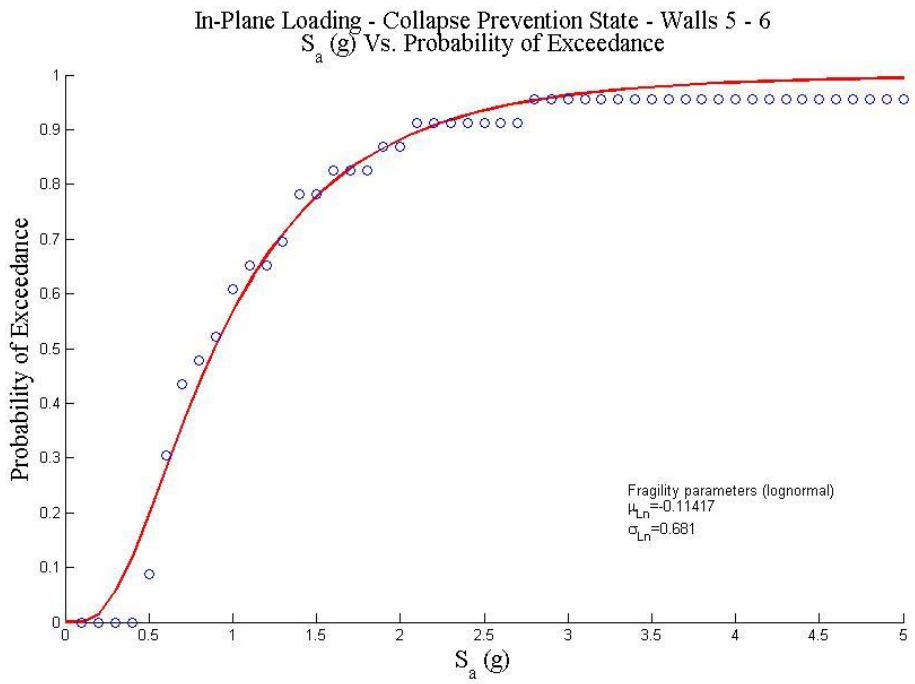


Figure 4.6 Fitted Fragility Curve for In-Plane Walls

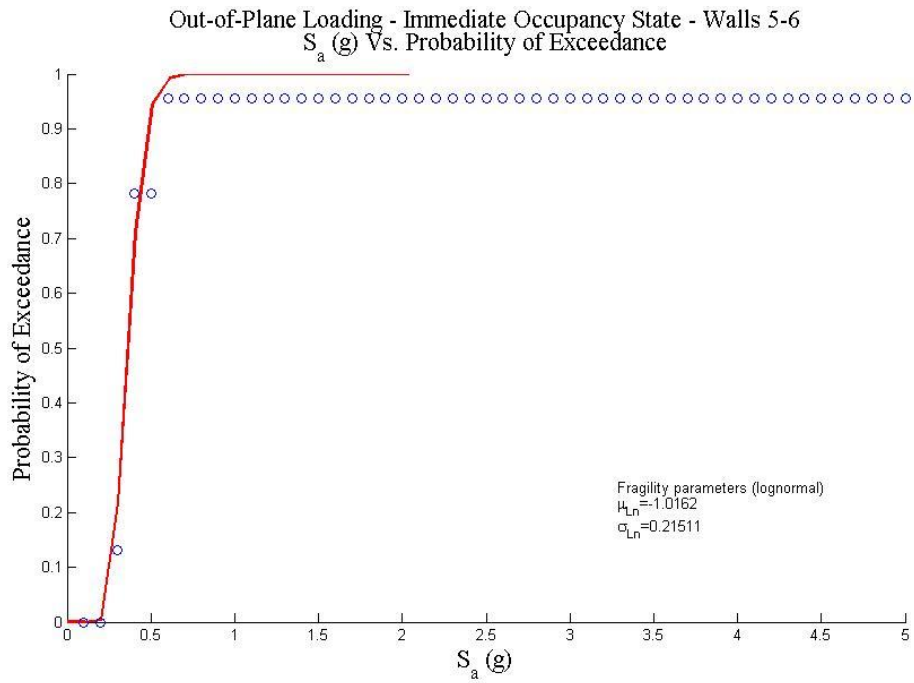


Figure 4.7 Fitted Fragility Curves for Out-of-Plane Walls

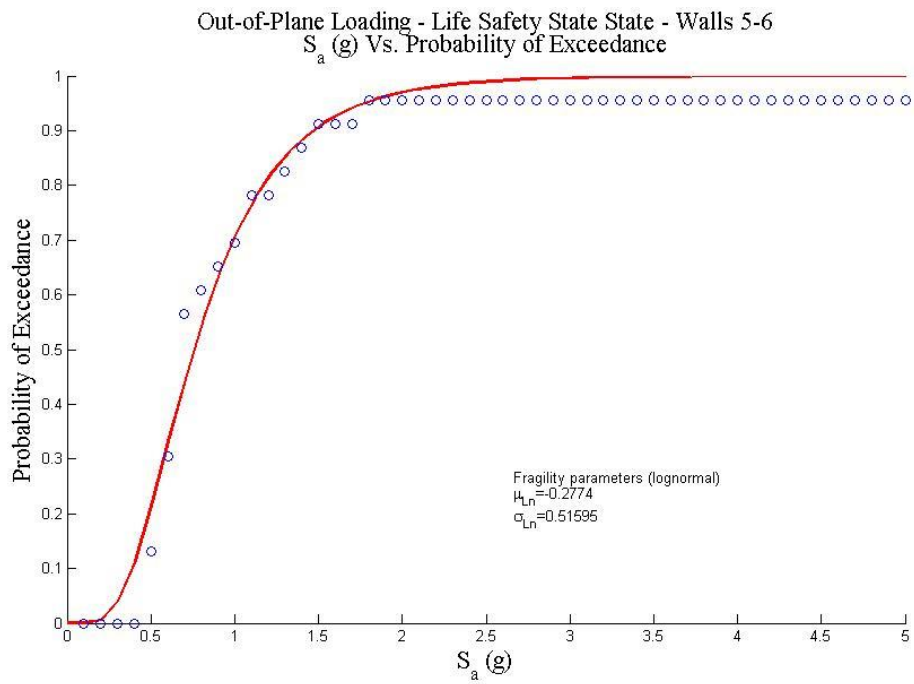


Figure 4.8 Fitted Fragility Curves for Out-of-Plane Walls

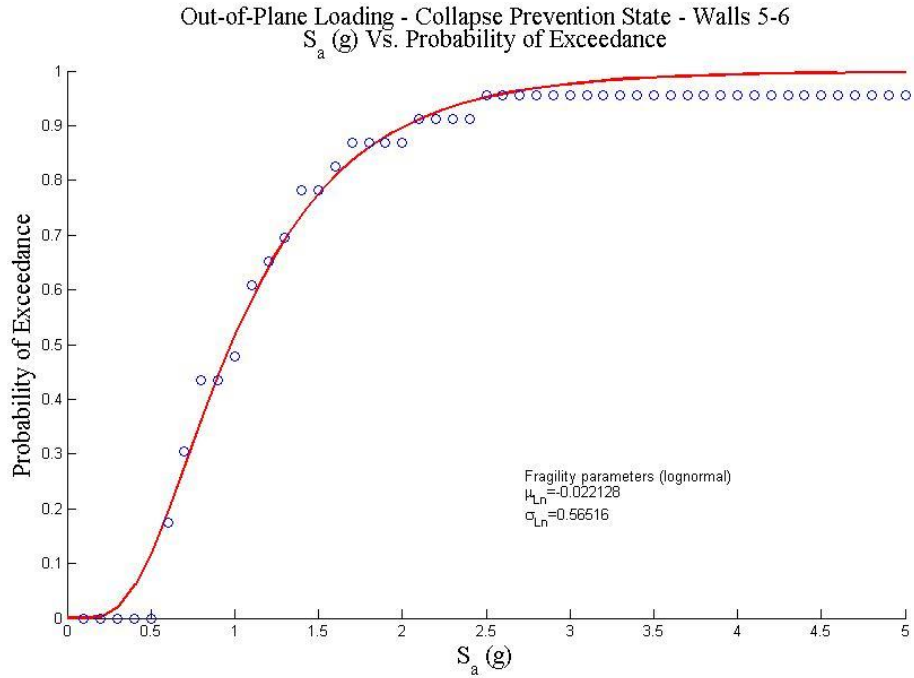


Figure 4.9 Fitted Fragility Curves for Out-of-Plane Walls

The probability of exceedance for the three limit states can be read from the fragility curves. Table 4.2 shows the probability of exceedance of limit states for three different earthquake levels for the walls 5 and 6 for models 1 and 2 respectively.

Table 4.2 Probability of Exceedance Damage Limit States

Cases	Spectral Acceleration (g)	Probability of Exceedance		
		Immediate Occupancy State	Life Safety State	Collapse Prevention State
Model 1	0.50	0.61	0.35	0.09
	0.76	0.87	0.57	0.43
	0.90	0.91	0.70	0.52
Model 2	0.50	0.74	0.13	0.00
	0.76	0.91	0.57	0.43
	0.90	0.91	0.70	0.52

4.4 Discussion

From the damage descriptions in Table 4.1 and the results showed in table 4.2, it can be stated that for the two cases of low rise masonry reinforced building mentioned in this study, both of them have more than 60% of probability of exceeding the Immediate Occupancy State at 0.5g of the scaled spectral acceleration. For the in – plane walls stated in Model 1, they have more than 30% of probability for exceeding the Life Safety State at 0.5g of the scaled spectral acceleration. For the out – of – plane walls stated on Model 2, they have more than 10% of probability of exceeding the Life Safety State compared at the same scaled spectral acceleration. Moreover, the probability of exceeding the Collapse Prevention State at 0.5g from the spectral acceleration is more than 8% for the in – plane walls and more than 40% for the out – of – plane walls showed in model 2.

Chapter 5: Conclusions

Model-based analytical fragility curves which define the probability of reinforced concrete masonry walls sustaining different states of damage, and therefore performance levels, in earthquakes of varying intensity have been presented in this study. The fragility curves were developed based on the hysteretic behavior obtained from existing quasi-static test data on reinforced concrete masonry walls. A simplified spring model was developed to describe the nonlinear dynamic behavior of reinforced masonry structures, and a typical low rise reinforced masonry building was modeled for the fragility analysis.

The fragility curves attained can show an adequate evaluation of the vulnerability or the probability of exceedance for low-rise masonry reinforced concrete structures under a given performance level in terms of the drift ratio.

The fragility curves also confirm that the out-of-plane walls are most vulnerable to damage by earthquakes in a reinforced masonry structure, mostly because the displacement suffered by an out-of-plane wall is higher than an in-plane wall, as one would anticipate. This reflects the importance of modeling out-of-plane walls in reinforced masonry structures for seismic risk analysis.

Further research could be conducted to extend the results of this research to multi-story reinforced concrete masonry structures. This research is related to low rise buildings only, and should be extended to multi-story buildings. Moreover, fragility curves could be developed incorporating different material properties and wall dimensions.

References

- American Society of Civil Engineers (ASCE). (2007). "Seismic Rehabilitation of Existing Buildings", American Society of Civil Engineers, Reston, Va.
- Aristizabals, J. C. (1999). Evaluation of a seismic damage parameter, *477*(November 1997).
- Bendimerad, F. (2001), "Loss Estimation: A Powerful Tool for Risk Assessment and Mitigation," *Soil Dynamics and Earthquake Engineering*, Vol. 21, pp. 467-472.
- Bernardini, A., Giuffre, A., and Modena, C. (1984). "Reinforced hollow clay brick masonry walls under seismic actions." *Proc., 8th World Conf. on Earthquake Engineering.*, Prentice-Hall, Englewood Cliffs, N.J.,4, 679-686.
- Calvi, G., Pinho, R., Magenes, G., Bommer, J., Restrepo-Velez, L. and Crowley, H. (2006), "Development of Seismic Vulnerability Assessment Methodologies Over the Past 30 Years," *Journal of earthquake Technology*, Vol. 43 pp. 75-104.
- Chandler, A. M. and Nelson, T. K. L. (2001), "Performance-Based Design in Earthquake Engineering: A Multi-Disciplinary Review," *Engineering Structures*, Vol. 23, pp. 1525-1543.
- Coburn, A. W., Spence, R. J. S., Pomonis, A. (1994), "Vulnerability and Risk Assessment," *Disaster Management Training Programme (DMTP) of the United Nations Development Programme (UNDP)*, Cambridge Architectural Research Limited, Cambridge, UK.
- EERI (1997), "Theme Issue: Loss Estimation" *Earthquake Spectra*, Vol. 13, No. 4.
- Folz, B., Asce, M., Filiatrault, A., & Asce, M. (2004a). *Seismic Analysis of Woodframe Structures . II : Model Implementation and Verification*, (September), 1361–1370.
- Folz, B., Asce, M., Filiatrault, A., & Asce, M. (2004b). *Seismic Analysis of Woodframe Structures. I: Model Formulation*, (September), 1353–1360.
- Foschi, R. O. (1977). "Analysis of wood diaphragms and trusses, Part 1: Diaphragms." *Can. J.. Civ. Engrg.*, Ottawa, 4(3), 345-362.
- Harris, J. R., Heintz, J. A., Manager, P., Hooper, J., Porush, A. R., Cranford, S., Haas, K., et al. (2009). *Quantification of Building Seismic Performance Factors*, (June).
- Huxtable A. (2004) *Frank Lloyd Wright*. New York.
- Kim, S.-C., & White, D. W. (2004). Nonlinear analysis of a one-story low-rise masonry building with a flexible diaphragm subjected to seismic excitation. *Engineering Structures*, 26(14), 2053–2067. doi:10.1016/j.engstruct.2004.06.008

- Kramer, S.L., (1996), *Geotechnical Earthquake Engineering*, Prentice Hall, NJ.
- McLean, D. I., Mcginley, W. M., Shing, P. B., & Diego, S. (2010). *Performance –Based Design of masonry and Masonry Veneer Final Internal Report to the National Science Foundation* by.
- Marcellini, A., Daminelli, R., Franceschina, G., and Pagani, M. (2001), “Regional and Local Seismic Hazard Assessment,” *Soil Dynamics and Earthquake Engineering*, Vol. 21, pp. 415-429.
- Orga-, I. S. (2001). *Cyclic Analysis of Wood Shear Walls*, (April), 433–441.
- Pang, W. C., Rosowsky, D. V, Asce, M., Pei, S., Lindt, J. W. Van De, & Asce, M. (2007). *Evolutionary Parameter Hysteretic Model for Wood Shear Walls*, (August), 1118–1129.
- Pang, W.C., Rosowsky, D., van de Lindt, J., and Pei, S. (2010) “Simplified direct displacement design of six-story neeswood capstone building and pre-test seismic performance assessment,” *ASCE Journal of Structural Engineering*, ASCE Library, 134: pp: 813-825, American Society of Civil Engineers.
- Park, J., Craig, J.I., Goodno, B.J., 2002, "Simple nonlinear in-plane response models for assessing fragility of URM walls," *7NCEE*, Boston, MA, July 21-25.
- Park, J., Towashiraporn, P., Craig, J. I., & Goodno, B. J. (2009). Seismic fragility analysis of low-rise unreinforced masonry structures. *Engineering Structures*, 31(1), 125–137. doi:10.1016/j.engstruct.2008.07.021
- Pei, S. (2010). *SAPWood for Windows*.
- Rosowsky, D., and Elligwood, B. (2002) “Performance-based engineering of wood frame housing: fragility analysis methodology.” *J. Struct. Eng.*, 128(1), 32-38.
- Shing, P., Schuller, M., and Hoskere, S. (1990) “In-Plane resistance of reinforced masonry shear walls,” *J. Struct. Eng.* 116, 619-640.
- Society, A. (n.d.). *ASCE 7-05 Minimum Design Loads for buildings and other Structures*.
- Standard, S. R. (n.d.). *Seismic Rehabilitation of Existing Buildings*,.
- Stewart, W.G. (1987). “The seismic design of plywood sheathed shear walls,” PhD thesis, University of Canterbury, Christchurch, New Zealand.
- Tanrikulu, A.K., Mengi, Y., and McNiven, H. D. (1992). “The nonlinear response of unreinforced masonry buildings to earthquake excitations.” *Earthquake Engrg and Struct. Dynamics*, 21(11), 965-985.

Tassios, T. (1984). "Behaviour of walls including infilled frames under cyclic loading," Proc., CIB Symp. On Wall Struct., Int. Ctr. for Build. Sys., Res. And Devel., Warsaw, Poland.

Wakabayashi, M. and Nakamura, T. (1984). "Reinforcing Principle and Seismic Resistance of Brick Masonry Walls," Proc., 8th World Conf. on Earthquake Engineering., Prentice-Hall, Englewood Cliffs, N.J., 5, 661-667.

Wong, K. K. F., & Wang, Y. (2001). Energy-Based Damage Assessment on Structures During Earthquakes, 154(January), 135–154.